Heliyon 8 (2022) e09181

Contents lists available at ScienceDirect

Heliyon

journal homepage: www.cell.com/heliyon

Research article

Enhanced light olefins production via *n*-pentane cracking using modified MFI catalysts

Ziyauddin S. Qureshi [a,*], Palani Arudra [a], M.A. Bari Siddiqui [a], Abdullah M. Aitani [a], Gazali Tanimu [a], Hassan Alasiri [a,b]

[a] Center for Refining & Advanced Chemicals, King Fahd University of Petroleum & Minerals, Dhahran 31261, Saudi Arabia
[b] Department of Chemical Engineering, King Fahd University of Petroleum & Minerals, Dhahran 31261, Saudi Arabia

HIGHLIGHTS

- *n*-pentane cracking over MFI zeolites with various Si_2O_3/Al_2O_3 ratios (30, 80, 280, 500, and 1500) was investigated.
- MFI (280) zeolite at 650 °C showed 51% selectivity for light olefins ($C_3^=/C_2^=$ = 0.7) with 23.8% undesirable C_2-C_4 alkanes.
- Phosphorous-modified large crystal MFI catalyst with moderate acid sites inhibited hydrogen transfer reaction.
- P/HZ280-LC provide improved light olefins production (selectivity 52.2%, $C_3^=/C_2^=$ = 1.3).

GRAPHICAL ABSTRACT

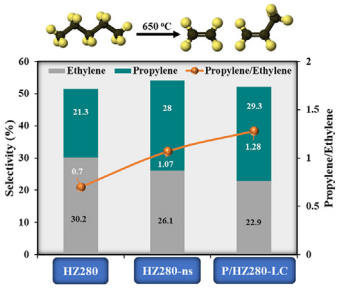

ARTICLE INFO

Keywords:
Catalytic cracking
n-pentane
Phosphorous-modified MFI
Olefins
Ethylene
Propylene

ABSTRACT

n-pentane catalytic cracking was studied over a series of MFI zeolites with varying SiO_2/Al_2O_3 ratios (30, 80, 280, 500, and 1500) using a fixed-bed reactor operated at temperature 550–650 °C. Other MFI zeolites (SiO_2/Al_2O_3 = 280) with various crystal morphology and size (such as large crystal and nano size) were also synthesized and tested for *n*-pentane cracking. The effects of MFI zeolite modification with ammonia and phosphorus on its physiochemical properties and catalytic activity were investigated. Among the parent MFI zeolites, MFI (280) demonstrated high selectivity (51%) towards light olefins ($C_3^=/C_2^=$ = 0.7) at 650 °C with undesired C_1–C_4 alkanes (38%). Surface modified MFI (280) zeolites of different crystal size and morphology showed improvement towards propylene selectivity by suppressing undesired reactions. Phosphorous-modified MFI zeolite with a large crystal size was found to improve light olefin selectivity (52.2%) with $C_3^=/C_2^=$ = ~1.3 and reduce undesired C_1–C_4 alkanes (8%) formation due to suppressed strong acidic sites. The characterization and evaluation results for the modified MFI (280) revealed that the incorporation of phosphorous created moderate acidic sites, which were stabilized by some non-framework aluminum species, thereby leading to suppressing the formation of undesired C_1–C_4 alkanes with improved light olefins selectivity.

* Corresponding author.
E-mail address: zqureshi@kfupm.edu.sa (Z.S. Qureshi).

https://doi.org/10.1016/j.heliyon.2022.e09181
Received 10 November 2021; Received in revised form 11 January 2022; Accepted 17 March 2022

1. Introduction

The rapid development of light olefins (propylene and ethylene) mostly in majority of polymer and petrochemical industries sparked attention for the development of novel catalytic production techniques using alkanes as the starting raw material [1, 2]. Propylene and ethylene are generally obtained from the steam pyrolysis/cracking of C_2–C_4 alkanes, and light naphtha at temperatures ranging from 800-1000 °C [1, 3]. The major constraint in steam cracking is high process temperature, which estimates for 40% of energy required for the global petrochemical industries [4, 5]. Light naphtha stream (mainly *n*-C_5 and *n*-C_6) has become an unfavorable gasoline blending component due to its high vapor pressure and low octane number [6]. Moreover, pyrolysis process leads to high amount of CO_2 liberation, a major contributor to global warming [7]. Thus, there is a need to find out a catalytic route to control the product distribution through mild operating conditions.

Some well-known catalytic conversion methods for producing light olefins include dehydrogenation of light alkanes (propane and ethane) [8], metathesis of alkenes (butene and ethylene) [9], methanol to olefin (MTO) [10, 11], and fluid catalytic cracking (FCC) [12]. Catalytic cracking of light alkanes (C_2–C_5) to produce ethylene and propylene is an efficient process due to their availability and low cost relative to the corresponding alkenes, thus resulting in an economic advantage [13]. Catalytic cracking reaction uses variety of hydrocarbon feed-stocks such as naphtha [14], heavy oil [15], and C_4/C_5 hydrocarbons [16], for producing light olefins. C_5 raffinate, a byproduct of FCC refinery streams and naphtha cracking is a potential source to make light olefins.

Several investigations were conducted on various types of zeolite frameworks for the production of light olefins from the cracking of *n*-pentane. Gruver et al. [17] cracked *n*-pentane over four series of dealuminated zeolites; HY (DHY), H-mordenite (DHM), MFI (DHZ) and fluorinated ultrastable Y (USYnF). It was revealed that, the selectivity to isomerization or cracking products depended on the zeolite structure. Cracking was enhanced over DHZ, whereas DHY and USYnF favored isomerization. The selectivity to isomerization in DHM was almost 50%. Hou et al. [18] investigated *n*-pentane cracking reactions over HZSM-35, H-Beta, and HZSM-5 zeolites. MFI zeolite demonstrated the greatest selectivity for light olefins, while Ag-incorporated MFI aided in C–H bond cleavage, hence increasing selectivity to light olefins. Thivasasith et al. [19] studied the effect of nano-cavities in different zeolite structures (H-FAU, H-ZSM-5, and H-FER) on the reaction mechanism for *n*-pentane cracking utilizing density functional measurements. Ethylene-propane and ethane-propylene activation energies differed by 0.5, 5.0, and 6.7 kcal mol^{-1}. It was concluded that using small pore zeolites (H-FER) results in a high propylene to ethylene ratio.

Recent literature studies for catalytic cracking of C_5 hydrocarbons using micro- and mesoporous MFI catalysts confirmed that, the existence of a unique pore shape and moderate acid sites resulted in higher light olefin yields [18, 20, 21]. Lee et al. [22] developed a range of micro- and mesoporous MFI catalysts using a carbon templating method (0–50 wt.%). The increased mesoporosity of the MFI catalysts, which enhanced reactant diffusion into the catalyst active sites, resulted in a high C_5 raffinate conversion (69%) and increased yield (40%) in light olefins.

Hou et al. [23] studied the impacts of regeneration of metal-modified MFI-based catalysts mostly on selectivity to light olefins. Regenerated Ag-MFI achieved 69 wt.% selectivity towards light olefins, which was approximately 25% higher than the parent MFI zeolite. At 500 °C light olefins yields of over metal-incorporated MFI catalysts (Zr, Ag) and regenerated MFI were 19.0%, 21.7%, and 25.6%, respectively, compared with yield over the parent MFI (12.0%) [24]. However, at 550 °C, the Zr-MFI catalyst exhibited an increase in light olefins production, which was related to increase in hydride transfer reactions resulting from the Brønsted acid sites thus improving catalytic performance. Cordero-Lanzac et al. [25] explored *n*-pentane cracking over Zr-incorporated MFI catalysts prepared via impregnation and chemical liquid deposition (CLD) method. Strong acid sites on the surface of surface modified MFI catalysts were significantly reduced, resulting in higher catalytic activity and improved selectivity for light olefins [26, 27].

In this study, *n*-pentane catalytic cracking was investigated to produce light olefins using a range of MFI zeolites of varying SiO_2/Al_2O_3 ratios (SAR). To improve selectivity towards propylene and suppress the undesirable reactions, MFI zeolite (SAR = 280) with different crystal sizes and morphologies were further investigated. The impact of surface modification by ammonia treatment and phosphorous loading on physiochemical properties and catalytic activities of *n*-pentane catalytic cracking to produce light olefins was reported.

2. Experimental procedure

2.1. Chemical reagents

98% pure tetrapropylammonium bromide, tetrapropylammonium hydroxide (40% aqueous solution), 99.99% aluminum sulfate hydrate, 98% pure anhydrous *n*-pentane, 99% pure tetraethyl orthosilicate, 98% pure ammonium fluoride, 99.8% pure fumed silica; obtained from Sigma-Aldrich and phosphoric acid (85% w/w) from Samchun Chem. were used without being purified any further.

2.2. Preparation of catalysts

Zeolyst International provided NH_4 form MFI zeolites with SAR (30, 80, 280, 500, and 1500). The parent zeolites were converted into H-form via calcination in air for 5 h at 550 °C. They are denoted as catalyst HZ30, HZ80, HZ280, HZ500, and HZ1500. Preparation methods of different MFI catalysts (SAR = 280) were used as reported previously and are denoted as HZ280-ns (ns: nano size), HZ280-LC (LC: large crystal), and HZ280-LC-NH_3 (ammonia modified) [28].

2.2.1. Nano size HZ280 catalyst

In a typical synthesis, fumed silica (12.0 g) was combined with tetrapropylammonium hydroxide (TPAOH, 3.46 g), aluminum sulfate (0.24 g) and water (13.4 g). The resultant mixture was transferred in a Teflon autoclave and hydrothermal crystallization was carried out for 4 days at 90 °C. The resulting gel had a total composition of 1.0 SiO_2/0.085 TPAOH/0.00357 Al_2O_3/3.72 H_2O. Following crystallization, obtained solid was centrifuged and washed thoroughly with deionized water three times. The resulting solid was dried overnight at 90 °C before being calcined at 750 °C for 6 h (heating rate 1 °C/min). The zeolite catalyst obtained using this method was designated as HZ280-ns.

2.2.2. Large crystal HZ280 catalyst

In a typical synthesis, tetrapropylammonium bromide (TPAB, 4.26 g), ammonium fluoride (0.74 g), and aluminum sulfate (0.24 g) have been dissolved in deionized water (72 mL). The obtained solution was then combined with fumed silica (12.0 g) until the formation of homogeneous gel. The resultant gel was transferred in Teflon autoclave and hydrothermal crystallization was carried out for 2 days at 200 °C. The resulting gel had a total molar composition of 1.0 SiO_2/0.08 TPAB/0.1 NH_4F/0.00357 Al_2O_3/20 H_2O. Following crystallization, obtained solid was washed thoroughly with adequate amount of deionized water, filtered and dried overnight at 80 °C before being calcined at 750 °C for 6 h in air to get rid of the template. The zeolite catalyst obtained using this method was designated as HZ280-LC.

2.2.3. Ammonia-modified large crystal HZ280 catalyst

Surface modification was accomplished in a glass beaker by combining 4 g of HZ280-LC with 20 g solution containing ammonium nitrate (10 g, 7.5 wt.%) and aqueous ammonia (10 g, 25 wt.%). The suspension was swirled for 1 h at 90 °C at autogenous pressure in a polypropylene bottle. The final solid was extensively washed using deionized water, dried for 4 h at 110 °C and calcined in air for 5 h at 550 °C. The ammonia-modified sample was denoted as HZ280-NH_3.

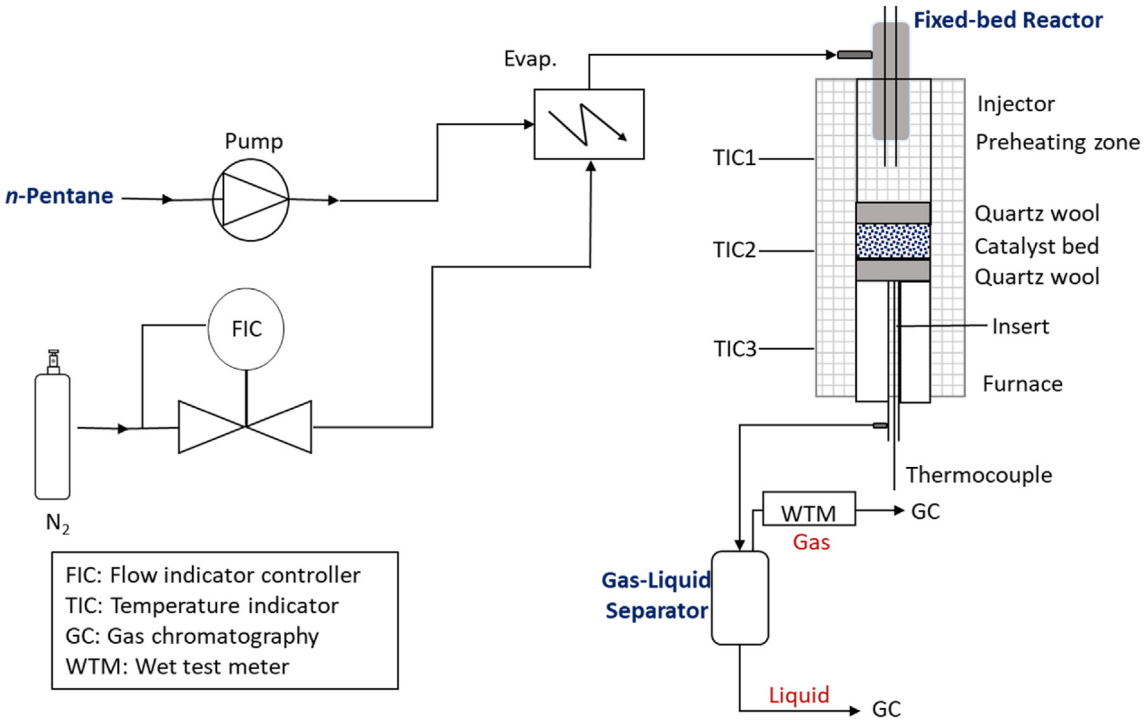

Figure 1. Schematic diagram of the fixed-bed reactor.

2.2.4. Phosphorous-modified large crystal HZ280 catalyst

The preparation of phosphorous-modified MFI catalyst was carried out by impregnation method. In 10 mL of deionized water a calculated amount of phosphoric acid (85% w/w) was dissolved. 3 g of HZ280-LC catalyst was disseminated in the phosphoric acid solution with steady mixing for 5 h at 40 °C. The solid material was then dried for 12 h at 100 °C before being calcined for 5 h at 650 °C. ICP-OES analysis indicated that 0.457 wt.% of P was deposited onto the P/HZ280-LC catalyst.

2.3. Catalyst characterization

The Rigaku Miniflex II instrument was used to analyze powdered X-ray diffraction (XRD) arrays of the catalyst samples utilizing Cu-Kα radiation with a wavelength, $\lambda = 1.5405$ Å and 30 kV, 15 mA operating parameters. A scanning angle of $2\theta = 5.0–60°$, step size of 0.02° and angular speed of 2°/min were utilized.

Phosphorous content was evaluated using Vario Micro Cube, Elementar inductively coupled plasma optical emission spectrometry (ICP-OES analysis). Micromeritics ASAP 2020 instrument was used in obtaining N_2 adsorption-desorption isotherms. The pore information and surface areas were computed using the Barret-Joyner-Halenda (BJH) method and Brunauer-Emmett-Teller (BET) equation, respectively.

The catalysts acidic property was determined with TGA, Mettler Toledo apparatus using the NH_3 temperature programmed desorption experiments. 0.05 g of the sample was weighed and pretreated at 300 °C for 2 h in a 25 mL/min He stream. The catalyst was cooled to 25 °C, and NH_3 gas (50 mL/min) was used to saturate the catalyst acid sites at 100 °C for 30 min. The physically adsorbed NH_3 was removed by heating at 120 °C for 2 h in a 50 mL/min He atmosphere. In a 25 mL/min He flow, the sample was allowed to cooled to 50 °C before being heated to 700 °C (10 °C/min). A thermal conductivity detector was used to detect the desorbed NH_3 (TCD).

Images of the catalysts samples were captured using a JEOL JSM-5800 scanning electron microscope (SEM) at a magnification of 17000. Under vacuum, the catalyst samples were covered with a thin layer of gold by using cressington sputter ion-coater operated at 15 mA current for 20 s.

2.4. Catalytic evaluation

In a fixed-bed tubular reactor system, *n*-pentane catalytic cracking was carried out (Figure 1). Main features of the reactor system comprise a feed section, pre-heating section, a once-through reactor and a separator section. The feed section consists of a metering pump to feed in liquid, a mass flow meter to measure gas feed. The reactor is a haste-alloy tube of 12-inch length and 10 mm ID. It is heated by a three-zone electrical furnace. The pre-heater zone consists of a stainless steel tube, heated by an electrical furnace. The reaction products were passed through a cooled jacketed vessel, to separate gaseous and liquid products. Gas products were analyzed off-line in an Agilent 3000A fast micro gas chromatograph. Liquid product is analyzed using an Agilent 5870 GC based detailed hydrocarbon analyzer, which works according to ASTM D6730.

After preheating to 250 °C, a pump delivered 2 cc/h of *n*-pentane into the reactor. Nitrogen was utilized as a carrier gas at 20 cc/min. 1.0 g of MFI catalyst (30–40 mesh size) was placed at the top half of a reactor tube, supported by quartz wool and a reactor insert. The reaction was carried out at atmospheric pressure, temperature ranging from 550-650 °C with a liquid hourly space velocity (LHSV) of 2.0 h^{-1} and a time-on-stream 1–4 h. The reactor temperature was raised to the required temperature before the feed was sent in. Reaction was allowed to take place for 60 min, when steady state was reached. The reaction products were passed through the separator, to separate gaseous and liquid products, which are collected for analysis.

Eqs. (1), (2), and (3) were used to calculate conversion (X) of *n*-pentane, yield (Y(i)) to species i and selectivity (S(i)) to species i.

$$X = 100 - (\text{Unreacted } n\text{-Pentane}) \tag{1}$$

$$Y(i) = \frac{Wi}{Wt\% \ \text{of} \ n - \text{Pentane}} \times 100 \tag{2}$$

$$S(i) = Y(i)/X \tag{3}$$

where, Wi weight (%) of species i.

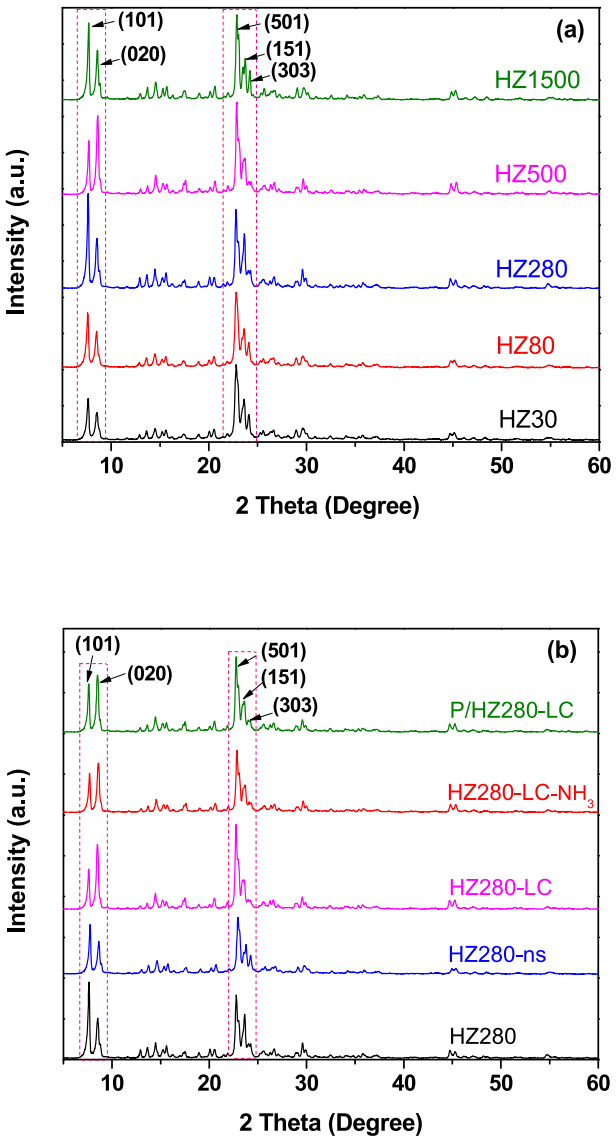

Figure 2. (a) XRD patterns of MFI zeolites with various SAR and (b) parent and modified HZ280 catalysts.

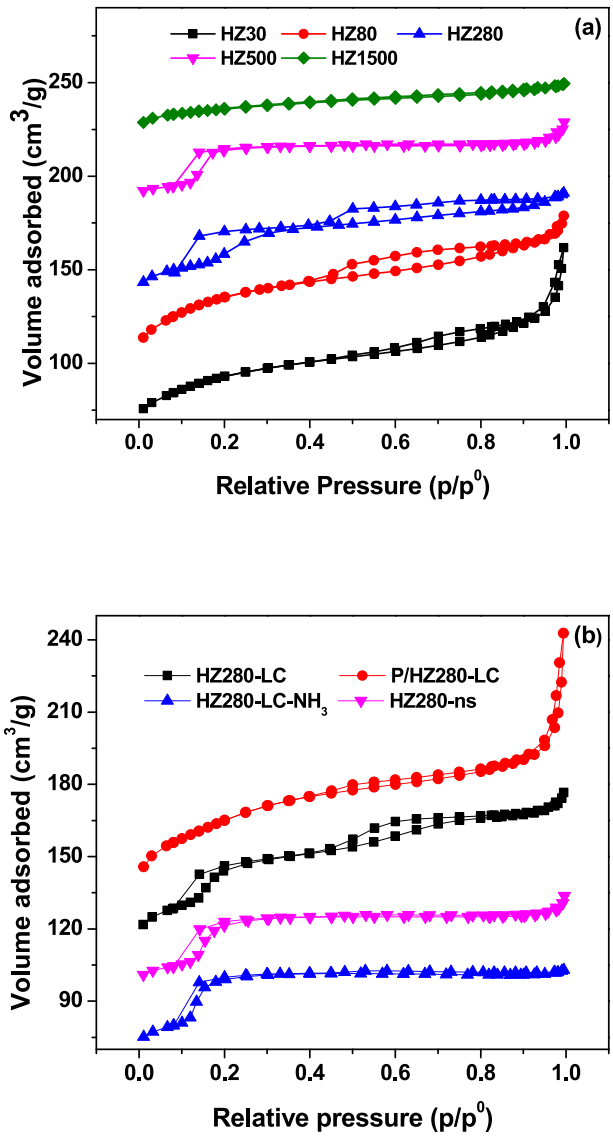

Figure 3. (a) N_2 adsorption-desorption isotherms of MFI zeolites with various SAR and (b) modified HZ280 catalysts.

3. Results and discussion

3.1. Characterization of the catalysts

Figure 2 presents XRD patterns for MFI catalysts with different SAR and modified HZ280 catalysts. All the catalysts in Figure 2(a) showed the typical MFI structure peaks in 2θ ranges of 7–10° and 22-25° [29]. Figure 2(b) depicts XRD pattern of the different modified MFI catalysts with SAR 280. The peak intensity at $2\theta = 7.4$ was higher than $2\theta = 8.5$ for HZ280 and HZ280-ns. However, it was reverse in the case of HZ280-LC catalysts. The presence of fluoride ion during large crystal synthesis promoted the formation of (020), (200), (−111) and (111) faces. Furthermore, no significant impurities other than sharp MFI characteristic peaks in XRD patterns were observed after HZ280 catalyst was modified with ammonia treatment and phosphorous loading.

Figure 3 displays the N_2 adsorption-desorption isotherms of parent and modified MFI catalysts. All the MFI catalysts show adsorption at very low pressures because of the interaction of the pore walls with the adsorbate, typical of microporous materials. Table 1 depicts the textural characteristics of parent and modified MFI catalysts. The surface area of parent MFI zeolites was measured using BET method, and it decreased as SAR increased from 80 to 1500. BET surface area of modified HZ280 catalysts was also influenced by surface modification with different methods. As expected BET surface area of HZ280-ns increased due to decrease in particle size and large surface area. For HZ280-LC catalyst

Table 1. Physiochemical properties of parent and modified MFI zeolites.

Catalyst	S_{BET} [m^2/g]	Pore vol. [cm^3/g]	Pore dia. [nm]	Amount NH_3 desorbed [mmol/g]		
				<300 °C	300–550 °C	Total Acidity
HZ30	351	0.17	4.68	1.12	0.53	1.65
HZ80	390	0.15	3.27	0.81	0.38	1.19
HZ280	359	0.18	2.17	0.24	0.12	0.36
HZ500	334	0.15	2.08	0.16	0.09	0.25
HZ1500	321	0.05	3.27	0.15	0.08	0.23
HZ280-ns	409	0.19	4.78	0.23	0.18	0.41
HZ280-LC	355	0.13	1.85	0.20	0.14	0.34
HZ280-LC-NH_3	332	0.17	2.47	0.25	0.13	0.38
P/HZ280-LC	327	0.13	2.04	0.19	0.11	0.30

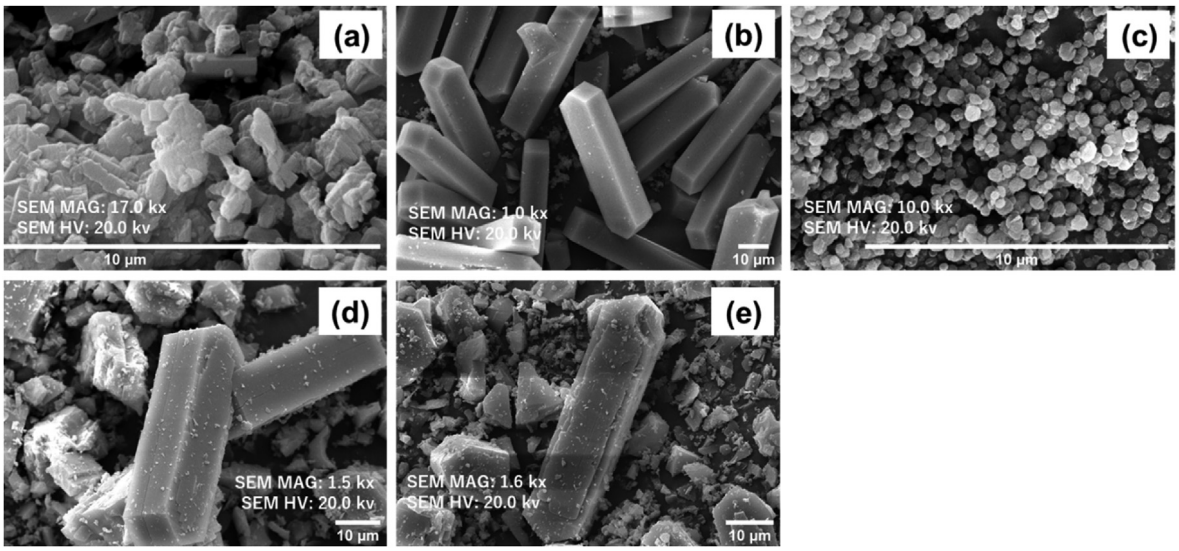

Figure 4. SEM images of (a) HZ280, (b) HZ280-LC, (c) HZ280-ns, (d) HZ280-LC-NH_3 and (e) P/HZ280-LC.

BET surface area decreased after the addition of phosphorous, which is ascribed to the destruction of some microspores, during phosphorous modification [30]. Average pore diameter increased with phosphorous loading which is attributed to the production of the mesopores caused by dealumination, thereby improving diffusion. Similar observation was also reported in the literature for phosphorous impregnated MFI catalyst [31].

SEM images of parent and modified HZ280 catalysts are presented in Figure 4(a-e). The SEM image of parent HZ280 (Figure 4a) shows relatively quadrangular prism-like crystallites. Figure 4b shows that the large crystal HZ280 zeolite represents a highly ordered large quadrangular prism-like crystallites morphology with large crystal size of about 40 µm HZ280-ns was observed to consist of only small spherical nanoparticles of average 300–400 nm crystal size (Figure 4c). After surface modification of HZ280-LC with 0.5 wt.% ammonia and phosphorous, a mixture of large crystallites with few small particles were observed, as shown in Figure 4d and e. The morphology revealed that P loading slightly damaged the structure of the MFI sample.

NH_3-TPD analysis were made to investigate the acid characteristics of parent and modified MFI zeolites, as shown in Table 1. Both the weak acidity (<300 °C) and strong acidity (300–550 °C) of MFI zeolites decreased with the increase of SAR. Furthermore, among the modified

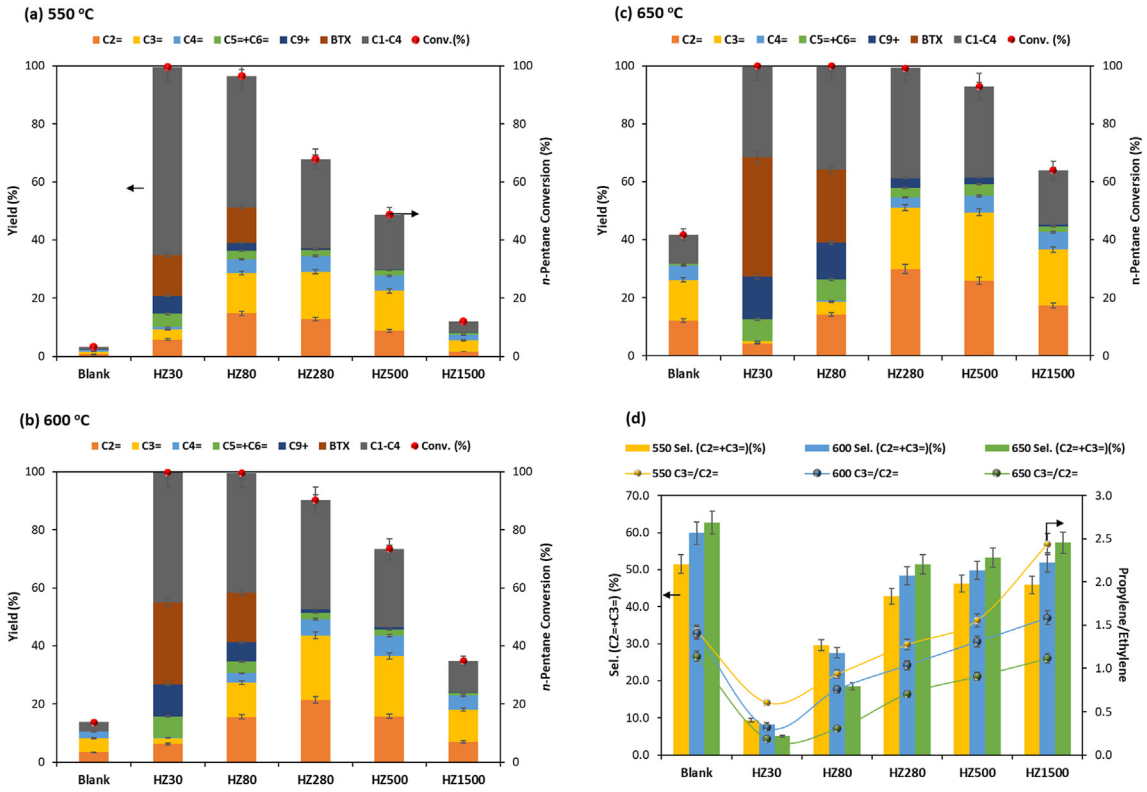

Figure 5. Temperature effects on *n*-pentane cracking and product distribution (a) 550 °C, (b) 600 °C, and (c) 650 °C; (d) ethylene and propylene selectivity and propylene/ethylene ratio for MFI catalysts with various SAR.

Table 2. Effect of temperature on *n*-pentane cracking and product distribution for MFI catalysts with various SAR.

Catalyst	Temp. (°C)	Conv. (%)	Yield (%)									Selectivity (%)	
			$C_2^=$	$C_3^=$	$C_2^=+C_3^=$	$C_4^= + C_4^{2=}$	$C_5^= + C_6^=$	C_1	$C_2–C_4$	BTX*	C_9+	$C_2^=$	$C_3^=$
Blank	550	3.3	0.7	1.0	1.7	0.5	0.1	0.3	0.6	0.0	0.1	21.2	30.3
	600	13.7	3.4	4.8	8.2	2.3	0.1	1.3	1.9	0.0	0.0	24.8	35.0
	650	41.6	12.2	13.9	26.1	4.9	0.7	5.0	4.9	0.0	0.0	29.3	33.4
HZ30	550	99.6	5.8	3.5	9.3	0.8	4.5	22.3	42.4	14.0	6.2	5.8	3.5
	600	99.8	6.3	2.0	8.3	0.2	7.3	20.9	23.9	28.2	11.0	6.3	2.0
	650	100.0	4.3	0.8	5.1	0.0	7.5	16.6	14.9	41.1	14.7	4.3	0.8
HZ80	550	96.4	14.8	13.8	28.5	4.8	2.9	6.4	38.8	12.2	2.7	15.4	14.3
	600	99.5	15.6	11.8	27.3	3.2	4.1	9.9	31.4	17.0	6.5	15.7	11.9
	650	100.0	14.2	4.3	18.5	0.5	7.3	15.2	20.6	25.2	12.6	14.2	4.3
HZ280	550	67.9	12.8	16.3	29.2	5.4	2.0	3.5	27.1	0.1	0.6	18.9	24.0
	600	90.2	21.4	22.2	43.5	5.6	2.2	6.8	30.7	0.0	1.3	23.7	24.6
	650	99.1	29.9	21.1	51.0	3.6	3.3	12.2	25.8	0.0	3.3	30.2	21.3
HZ500	550	48.7	8.8	13.7	22.5	5.2	1.9	2.5	16.3	0.0	0.3	18.1	28.1
	600	73.3	15.8	20.7	36.5	7.0	2.1	4.9	22.1	0.0	0.8	21.6	28.2
	650	92.8	25.9	23.5	49.4	5.7	4.1	9.6	21.7	0.0	2.3	27.9	25.3
HZ1500	550	12.0	1.6	3.9	5.4	1.9	0.7	0.7	3.1	0.0	0.1	13.3	32.5
	600	34.8	7.0	11.1	18.1	4.8	1.0	2.7	8.1	0.0	0.2	20.1	31.9
	650	63.9	17.3	19.3	36.6	6.0	1.9	7.5	11.4	0.0	0.6	27.1	30.2

* BTX = Benzene, toluene, xylenes, LHSV = 2 h^{-1}, TOS = 1 h.

HZ280 catalysts, the ammonia-modified catalyst exhibited an increase in total acidity (0.41 mmol/g). The increase in acidity is related to the enhancement of silanol group upon treatment with ammonia [32]. Moreover, P modified HZ280 reduced its strong acidity and total acidity as a results of dealumination from the tetrahedral framework aluminum, indicating that phosphorus was more related with the acidic sites of the HZ280 zeolite. Ji et al. [33] proposed that a significant number of weak acid sites over the surface of zeolite catalyst are required for the viable conversion of *n*-dodecane to produce light olefins. Strong acid sites in high concentrations may be accountable for the formation of undesirable products such as lower alkanes and aromatics [34]. It was clear from NH_3-TPD experiments that, the number of weak and strong acid sites is essential for the production of light olefins. According to Blasco et al. [34] an interaction exists between phosphorus and the acid sites corresponding to Al pair framework. This stabilizes the aluminum and varies the acidic property. Cracking is mainly enhanced on strong acid sites,

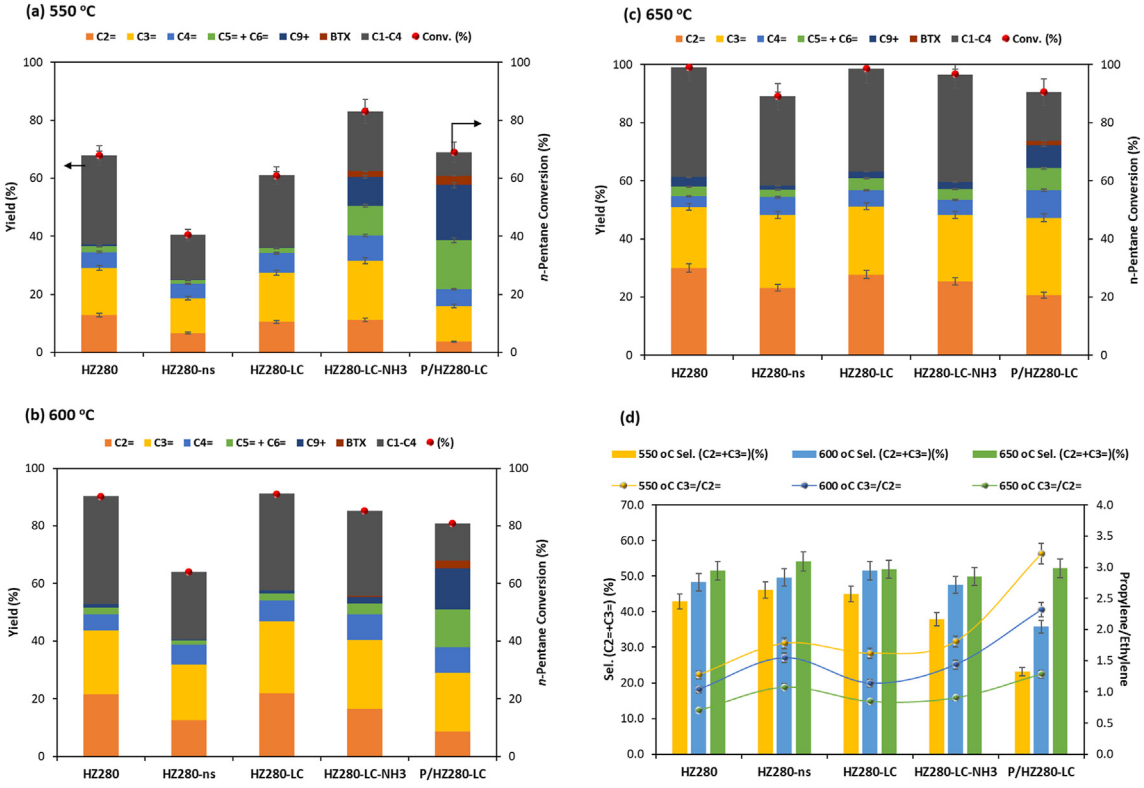

Figure 6. Temperature effects on *n*-pentane cracking and product distribution (a) 550 °C, (b) 600 °C, and (c) 650 °C; (d) propylene and ethylene selectivity and propylene/ethylene ratio for modified HZ280 catalysts.

Table 3. Effect of temperature on *n*-pentane cracking and product distribution over modified HZ280 zeolites.

Catalyst	Temp. (°C)	Conv. (%)	Yield (%)								Selectivity (%)		
			$C_2^=$	$C_3^=$	$C_2^=+C_3^=$	$C_4^= + C_4^{2=}$	$C_5^= + C_6^=$	C_1	C_2–C_4	BTX*	C_9+	$C_2^=$	$C_3^=$
HZ280	550	67.9	12.8	16.3	29.1	5.4	2	3.5	27.1	0.1	0.6	18.9	24.0
	600	90.2	21.4	22.2	43.6	5.7	2.2	6.8	30.8	0	1.3	23.7	24.6
	650	99.1	29.9	21.1	51	3.6	3.3	12.2	25.7	0	3.3	30.2	21.3
HZ280-ns	550	40.4	6.7	11.9	18.6	5	1.2	2	13.3	0	0.3	16.6	29.5
	600	64.1	12.5	19.3	31.8	7	1.4	4.1	19.4	0	0.3	19.5	30.1
	650	89	23.2	24.9	48.1	6.3	2.5	9	21.7	0	1.4	26.1	28.0
HZ280-LC	550	60.9	10.5	16.9	27.4	6.8	1.6	3.4	21.5	0	0.3	17.2	27.8
	600	91	21.9	24.9	46.8	7.2	2.6	6.7	26.8	0	1	24.1	27.4
	650	98.6	27.7	23.5	51.2	5.5	4.1	11.6	23.8	0	2.4	28.1	23.8
HZ280-LC-NH_3	550	83.1	11.2	20.3	31.5	8.8	10.2	2.7	17.9	1.9	10	13.5	24.4
	600	85.1	16.6	23.8	40.4	8.8	3.8	5.4	24	0.4	2.3	19.5	28.0
	650	96.7	25.3	22.9	48.2	5.2	3.8	11.3	25.6	0	2.4	26.2	23.7
P/HZ280-LC	550	68.9	3.8	12.2	16	5.8	16.8	1.2	6.8	3.3	19	5.5	17.7
	600	80.8	8.7	20.2	28.9	9	13	2.8	10	2.7	14.4	10.8	25.0
	650	90.5	20.7	26.5	47.2	9.5	7.6	7.2	9.7	1.4	8	22.9	29.3

* BTX = Benzene, toluene, xylenes, LHSV = 2 h^{-1}, TOS = 1 h.

thereby producing by-products and eventual coke deposition. As a consequence of the phosphorus modification, the acid amount over P/HZ280-LC catalyst decreased to 0.3 mmol/g, which helped *n*-pentane from over-cracking, reduced carbon deposition, and avoided blockage of zeolite micropores. As a result, the access of the reactants to the micropores and subsequent reaction on the acid sites became unrestricted [35].

Furthermore, phosphorous content of P/HZ280-LC catalyst was determined using ICP-OES analysis. It was found to be 0.457 wt.%, which matches the designed value, indicating successful impregnation of P in HZ280-LC catalyst.

3.2. *n*-Pentane catalytic cracking using MFI zeolites

3.2.1. Blank experiments

The experiments were conducted in a blank reactor containing only SiC (1.0 g) as diluent using the following conditions: *n*-pentane: 2.1 cc/h; N_2: 20 cc/h; atmospheric pressure; temperature: 550–650 °C. The results obtained for the blank test are presented in Figure 5 and Table 2 *n*-Pentane conversion at 550, 600, and 650 °C was found to be approximately 3.3, 13.7, and 41.6 wt.%, respectively. At 650 °C, yield of light olefins (propylene and ethylene) was 26.1 wt.%, by around 10 wt.% alkanes (C_1–C_4) (Figure 5c).

3.2.2. Influence of SiO_2/Al_2O_3 ratio

The performance of MFI catalysts with SAR from 30 to 1500 at 550–650 °C was carried out. The conversion of *n*-pentane and the detailed product distributions are summarized in Figure 5 and Table 2. The major reaction pathways over MFI catalysts are cracking, hydrogen transfer and cyclization resulting in the formation light olefins, alkanes and aromatics. In the blank experiment reaction conditions, *n*-pentane cracking towards light olefins was not significant. This shows that acidic sites are necessary for higher *n*-pentane conversion. The conversion of *n*-pentane decreased as SAR increased. Catalysts with low SAR had more acidic sites than catalysts with higher SAR. When compared to other catalysts, HZ30 and HZ80 catalysts with total acidity of 1.65 and 1.19 mmol/g increased the production of benzene, toluene, xylenes (BTX) and higher C9+ aromatics. It is well known that, over MFI catalyst, the yield of aromatics increases with reduction in SAR [36, 37]. MFI catalysts having lower SAR (high acidic sites) at 650 °C also gave rise to undesired alkanes like C_1–C_4 hydrocarbons from 18.9 % (SAR 1500) to 31.5% (SAR 30), as shown in Figure 5c. This is attributed to cracking followed by hydrogen transfer reaction (Table 2). Furthermore, as the acid sites were reduced, the aromatic yield decreased from 41.1% (SAR 30) to 0 % (SAR 1500). This reveals that the aromatic products formation proceeded through cracking followed by hydrogen transfer reaction, which require strong acid sites. Suppression of strong acid sites minimizes the degree of the hydrogen transfer reaction and, as a consequence increases ethylene and propylene yield. An enhanced production of light olefins is caused by moderate acid sites. Interestingly, HZ280 catalyst is the most active catalyst, not only in suppressing the undesired hydrogen transfer reaction but also producing the highest yield of ethylene and propylene (51%) having a propylene/ethylene ratio of 0.7 and 38% yield of C_1–C_4 hydrocarbons, as shown in Figure 5c, d.

3.2.3. Modified MFI (HZ280) catalysts

The primary objective of *n*-pentane cracking over modified catalyst is the formation of ethylene and propylene. Modifications of the HZ280 catalyst were made in particular to suppress the strong acid sites, thereby decreasing reactions caused by hydrogen transfer and resulting in the formation of lower alkanes (C_2–C_4). Figure 6a–c and Table 3 displayed

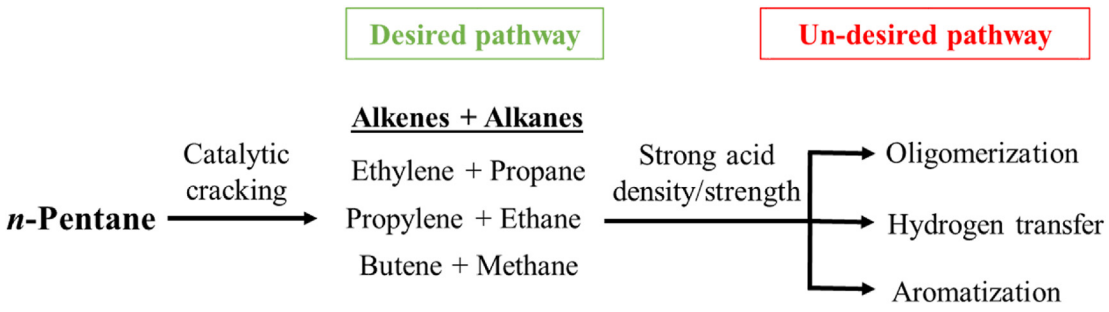

Scheme 1. Possible *n*-pentane catalytic cracking pathways.

the conversion of *n*-pentane, product yields over modified HZ280 catalysts (HZ280, HZ280-ns, HZ280-LC, HZ280-LC-NH_3, and P/HZ280-LC) at different reaction temperatures (550, 600, and 650 °C). Figure 6d compares the total selectivity for light olefins (propylene and ethylene), and propylene/ethylene ratio, for various modified HZ280 catalysts at temperatures ranging from 550 to 650 °C.

In general, thermal cracking favors the formation of ethylene, whereas catalytic cracking improves the formation of propylene. It was observed that, all modified HZ280 catalysts exhibited very good *n*-pentane conversion (89–99.1%) at 650 °C (Figure 6c). Among HZ280 zeolites with different crystal morphologies, such as nano size and large crystal, HZ280-LC showed a higher *n*-pentane conversion (98.6%) as well as an increased yield of light olefins (51.2%). However, after 1 h of reaction at 650 °C, the conversion was identical to that of HZ280 catalyst. When HZ280-LC-NH_3 was compared to the parent HZ280-LC, light olefins selectivity remained nearly identical with propylene/ethylene ratio at ~0.9 at 650 °C.

The phosphorous-modified HZ280-LC catalyst demonstrated a significant decrease in the yield of lower alkanes (C_2–C_4) 9.7% at 650 °C (Table 3). It was the lowest yield among the modified HZ280 catalysts. P/HZ280-LC showed improved propylene selectivity with propylene/ethylene ratio ~1.3 and good yield of light olefins (47.2%). This is mainly due to the catalyst's moderate acidity, which favored catalytic performance in terms of suppressing lower alkane formation (C_2–C_4), and higher yield of light olefins. Lee et al. [27] noticed a similar trend in which MFI zeolite with phosphorous treatment not only reduced strong acidity of the catalyst but also improved catalyst stability in catalytic cracking of C_5 raffinate.

3.2.4. Light olefins formation

The propylene to ethylene ratio revealed that propylene selectivity dependent on the kind of feedstock and reaction conditions. Figures 5d, 6d presents the propylene/ethylene ratio for MFI catalysts with different SAR and modified HZ280 catalysts at different reaction temperatures (550, 600, and 650 °C). The propylene/ethylene ratio for MFI catalysts with varying SAR was 2.4–1.6 at temperatures ranging from 550 to 600 °C. However, modified HZ280 catalysts demonstrated a propylene to ethylene ratio of 3.2–2.3, which decreased to about 1.3 at 650 °C. Propylene has been reported to be catalytically generated by the β-scission of long chain saturated hydrocarbons [38]. Because cracking aided by catalysts predominate at reduced temperatures (500–550 °C), an enhanced propylene yield was obtained as compared to ethylene. It is interesting to note that, even at a higher reaction temperature (650 °C), P/HZ280-LC catalyst favored catalytic cracking reaction resulting in improved propylene to ethylene ratio (~1.3). The results of *n*-pentane cracking reactions showed an enhanced propylene selectivity for the phosphorous-modified HZ280-LC due to moderate acidity.

As shown in Scheme 1, catalytic cracking of alkanes includes both desired and undesirable reaction pathways. Catalytic cracking of *n*-pentane produces smaller species such as alkane and alkene, which is a desired reaction pathway. Furthermore, because zeolite has a high acid density and acid strength, undesirable side reactions like as oligomerization, isomerization, and aromatization occur frequently [39]. As a consequence, selectivity to light olefins, and there is a large concentration of an undesirable product, giving rise to coke species [21]. As a consequence, in order to improve selectivity toward light olefins, unwanted pathways must be suppressed.

4. Conclusions

A series of MFI zeolites having SAR (30, 80, 280, 500, and 1500), different crystal sizes (HZ280-ns, HZ280-LC) and surface modified zeolite (P/HZ280-LC, HZ280-LC-NH_3) were synthesized, characterized and tested for *n*-pentane cracking. Among the parent MFI catalysts, HZ280 showed highest yield of light olefins, along with undesired alkanes due to cracking accompanied by hydrogen transfer reaction. Controlling the acid sites in the catalyst can often be used to reduce hydrogen transfer reactions. Among different crystal sizes of HZ280 catalyst, the larger crystal size catalyst showed improved *n*-pentane conversion (98.6%) and light olefins selectivity ($C_3^=/C_2^= = \sim 0.85$) compared to nano size catalyst (conversion 89%, $C_3^=/C_2^= = \sim 1.07$). The larger crystal size HZ280-LC catalyst had less density of acid sites, which suppressed the hydrogen transfer reactions. Modification with phosphorous on HZ280-LC catalyst, reduced strong acid sites further and enhanced light olefin selectivity 52.2% with $C_3^=/C_2^= = \sim 1.3$ and minimal formation of C_2–C_4 (8%) hydrocarbons.

Declarations

Author contribution statement

Ziyauddin S. Qureshi: Conceived and designed the experiments; Performed the experiments; Analyzed and interpreted the data; Wrote the paper.

Palani Arudra, M. A. Bari Siddiqui: Performed the experiments; Analyzed and interpreted the data; Contributed reagents, materials, analysis tools or data.

Abdullah M. Aitani: Conceived and designed the experiments; Analyzed and interpreted the data; Wrote the paper.

Gazali Tanimu: Performed the experiments; Contributed reagents, materials, analysis tools or data; Wrote the paper.

Hassan Alasiri: Conceived and designed the experiments; Contributed reagents, materials, analysis tools or data; Wrote the paper.

Funding statement

This work was supported by King Fahd University of Petroleum & Minerals, Dhahran, Saudi Arabia.

Data availability statement

Data included in article/supplementary material/referenced in article.

Declaration of interests statement

The authors declare no conflict of interest.

Additional information

No additional information is available for this paper.

Acknowledgements

The authors express their thanks to King Fahd University of Petroleum & Minerals (KFUPM), Dhahran, Saudi Arabia for the support in publishing this paper.

References

[1] N. Rahimi, R. Karimzadeh, Catalytic cracking of hydrocarbons over modified ZSM-5 zeolites to produce light olefins: a review, Appl. Catal. A: Gen. 398 (2011) 1–17.
[2] I. Amghizar, L.A. Vandewalle, K.M. Van Geem, G.B. Marin, New trends in olefin production, Engineering 3 (2017) 171–178.
[3] A.M. Aitani, Encyclopedia Chemical Processing, 2006, pp. 2461–2466.
[4] S.Y. Han, C.W. Lee, J.R. Kim, N.S. Han, W.C. Choi, C.H. Shin, Y.K. Park, Selective formation of light olefins by the cracking of heavy naphtha, in: Carbon Dioxide Utilization for Global Sustainability: Proceedings of the 7th International Conference on Carbon Dioxide Utilization, Seoul, Korea, 12–16th October (2003),, Elsevier, 2004, pp. 157–160.
[5] T. Ren, M. Patel, K. Blok, Olefins from conventional and heavy feedstocks: energy use in steam cracking and alternative processes, Energy 31 (2006) 425–451.
[6] A. Aitani, M.N. Akhtar, S. Al-Khattaf, Y. Jin, O. Koseoglu, M.T. Klein, Catalytic upgrading of light naphtha to gasoline blending components: a mini review, Energy Fuels 33 (2019) 3828–3843.
[7] Y. Wei, Z. Liu, G. Wang, Y. Qi, L. Xu, P. Xie, Y. He, Production of light olefins and aromatic hydrocarbons through catalytic cracking of naphtha at lowered temperature, Stud. Surf. Sci. Catal. 158B (2005) 1223–1230.

[8] O.V. Buyevskaya, D. Wolf, M. Baerns, Ethylene and propene by oxidative dehydrogenation of ethane and propane: performance of rare-earth oxide-based catalysts and development of redox-type catalytic materials by combinatorial methods, Catal. Today 62 (2009) 91–99.

[9] J.C. Mol, Industrial applications of olefin metathesis, J. Mol. Catal. A: Chem. 213 (2004) 39–45.

[10] M. Stöcker, Methanol-to-hydrocarbons: catalytic materials and their behavior, Microporous Mesoporous Mater. 29 (1999) 3–48.

[11] Z.M. Cui, Q. Liu, W.G. Song, L.J. Wan, Insights into the mechanism of methanol-to-olefin conversion at zeolites with systematically selected framework structures, Angew. Chem. Int. Ed. 45 (2006) 6512–6515.

[12] X. Gao, Z. Tang, D. Ji, H. Zhang, Modification of ZSM-5 zeolite for maximizing propylene in fluid catalytic cracking reaction, Catal. Commun. 10 (2009) 1787–1790.

[13] Z. Nawaz, Light alkane dehydrogenation to light olefin technologies: a comprehensive review, Rev. Chem. Eng. 31 (2015) 413–436.

[14] J. Wan, Y. Wei, Z. Liu, B. Li, Y. Qi, M. Li, P. Xie, S. Meng, Y. He, F. Chang, A ZSM-5-based catalyst for efficient production of light olefins and aromatics from fluidized-bed naphtha catalytic cracking, Catal. Lett. 124 (2008) 150–156.

[15] L. Zhao, J. Gao, C. Xu, B. Shen, Alkali-treatment of ZSM-5 zeolites with different SiO_2/Al_2O_3 ratios and light olefin production by heavy oil cracking, Fuel Process. Technol. 92 (2011) 414–420.

[16] O. Bortnovsky, P. Sazama, B. Wichterlova, Cracking of pentenes to C_2–C_4 light olefins over zeolites and zeotypes: role of topology and acid site strength and concentration, Appl. Catal. A: Gen. 287 (2005) 203–213.

[17] V. Gruver, Y. Hong, A.G. Panov, J.J. Fripiat, Role of Brønsted and Lewis acidity in the conversion of *n*-pentane on dealuminated H-Y, H-mordenite and HZSM-5, Stud. Surf. Sci. Catal. 101 (1996) 741–750.

[18] X. Hou, Y. Qiu, X. Zhang, G. Liu, Analysis of reaction pathways for n-pentane cracking over zeolites to produce light olefins, Chem. Eng. J. 307 (2017) 372–381.

[19] A. Thivasasith, T. Maihom, S. Pengpanich, C. Wattanakit, Nanocavity effects of various zeolite frameworks on n-pentane cracking to light olefins: combination studies of DFT calculations and experiments, Phys. Chem. Chem. Phys. 21 (2019) 22215–22223.

[20] X. Feng, G. Jiang, Z. Zhao, L. Wang, X. Li, A. Duan, J. Liu, C. Xu, J. Gao, Highly effective F-modified HZSM-5 catalysts for the cracking of naphtha to produce light olefins, Energy Fuels 24 (2010) 4111–4115.

[21] C. Rodaum, A. Thivasasith, D. Suttipat, T. Witoon, S. Pengpanich, C. Wattanakit, Modified acid-base ZSM-5 derived from core-shell ZSM-5@aqueous miscible organic-layered double hydroxides for catalytic cracking of n-pentane to light olefins, ChemCatChem 12 (2020) 4288–4296.

[22] J. Lee, U.G. Hong, S. Hwang, M.H. Youn, I.K. Song, Production of light olefins through catalytic cracking of C_5 raffinate over carbon-templated ZSM-5. Fuel Process, Technol. 108 (2013) 25–30.

[23] X. Hou, Y. Qiu, X. Zhang, G. Liu, Effects of regeneration of ZSM-5 based catalysts on light olefins production in n-pentane catalytic cracking, Chem. Eng. J. 321 (2017) 572–583.

[24] X. Hou, Y. Qiu, E. Yuan, F. Li, Z. Li, S. Ji, Z. Yang, G. Liu, X. Zhang, Promotion on light olefins production through modulating the reaction pathways for n-pentane catalytic cracking over ZSM-5 based catalysts, Appl. Catal. A: Gen. 543 (2017) 51–60.

[25] T. Cordero-Lanzac, A.T. Aguayo, A.G. Gayubo, P. Castaño, J. Bilbao, Simultaneous modeling of the kinetics for n-pentane cracking and the deactivation of a HZSM-5 based catalyst, Chem. Eng. J. 331 (2018) 818–830.

[26] N. Rahimi, D. Moradi, M. Sheibak, E. Moosavi, R. Karimzadeh, The influence of modification methods on the catalytic cracking of LPG over lanthanum and phosphorus modified HZSM-5 catalysts, Microporous Mesoporous Mater. 234 (2016) 215–223.

[27] J. Lee, U.G. Hong, S. Hwang, M.H. Youn, I.K. Song, Catalytic cracking of C_5 raffinate to light olefins over phosphorous-modified microporous and mesoporous ZSM-5, J. Nanosci. Nanotechnol. 13 (2013) 7504–7510.

[28] P. Arudra, T.I. Bhuiyan, M.N. Akhtar, A.M. Aitani, S.S. Al-Khattaf, H. Hattori, Silicalite-1 as efficient catalyst for production of propene from 1-butene, ACS Catal. 4 (2014) 4205–4214.

[29] M.M.J. Treacy, J.B. Higgins, R. von Ballmoos, Collection of Simulated XRD Powder Patterns for Zeolites, Elsevier, New York, 1996, p. 523.

[30] N. Xue, X. Chen, L. Nie, X. Guo, W. Ding, Y. Chen, M. Gu, Z. Xie, Understanding the enhancement of catalytic performance for olefin cracking: hydrothermally stable acids in P/HZSM-5, J. Catal. 248 (2007) 20–28.

[31] G. Zhao, J. Teng, Z. Xie, W. Jin, W. Yang, Q. Chen, Y. Tang, Effect of phosphorus on HZSM-5 catalyst for C_4-olefin cracking reactions to produce propylene, J. Catal. 248 (2007) 29–37.

[32] W.F. Hoelderich, J. Roeseler, G. Heitmann, A.T. Liebens, The use of zeolites in the synthesis of fine and intermediate chemicals, Catal. Today 37 (1997) 353–366.

[33] Y. Ji, H. Yang, Q. Zhang, W.J. Yan, Phosphorus modification increases catalytic activity and stability of ZSM-5 zeolite on supercritical catalytic cracking of n-dodecane, Solid State Chem. 251 (2017) 7–13.

[34] T. Blasco, A. Corma, J.M. Triguero, Hydrothermal stabilization of ZSM-5 catalytic-cracking additives by phosphorus addition, J. Catal. 237 (2006) 267–277.

[35] C.H.L. Tempelman, E.J.M. Hensen, On the deactivation of Mo/HZSM-5 in the methane dehydroaromatization reaction, Appl. Catal. B Environ. 176–177 (2015) 731–739.

[36] J.L. Hodala, A.B. Halgeri, G.V. Shanbhag, R.S. Reddy, N.V. Choudary, P.V.C. Rao, M.G. SriGanesh, G. Shah, R. Ravishankar, Aromatization of C_5-rich light naphtha feedstock over tailored zeolite catalysts: comparison with model compounds (n-C_5 - n-C_7), ChemistrySelect 1 (2016) 2515–2521.

[37] A. Abdalla, P. Arudra, S.S. Al-Khattaf, Catalytic cracking of 1-butene to propylene using modified H-ZSM-5 catalyst: a comparative study of surface modification and core-shell synthesis, Appl. Catal., A 533 (2017) 109–120.

[38] F. Jentoft, B.C. Gates, Solid-acid-catalyzed alkane cracking mechanisms: evidence from reactions of small probe molecules, Top. Catal. 4 (1997) 1–13.

[39] C. Rodaum, A. Thivasasith, P. Iadrat, P. Kidkhunthod, S. Pengpanich, C. Wattanakit, Ge-Substituted hierarchical ferrierite for n-pentane cracking to light olefins: mechanistic investigations via in-situ DRIFTS studies and DFT calculations, ChemCatChem 14 (3) (2021).